



Structural damage detection of reinforced concrete shear walls subject to consequent earthquakes

F. Khademian¹ · H. Naderpour¹  · M. K. Sharbatdar¹Received: 16 November 2019 / Accepted: 11 December 2019 / Published online: 16 December 2019
© Springer Nature Switzerland AG 2019

Abstract

Structural health monitoring is a procedure to provide accurate and immediate information on the condition and efficiency of structures. There is a variety of damage factors and the unpredictability of future damage, is essential for the application of structural health monitoring. Structural health monitoring and damage detection in early stages is one of the most fascinating topics that had been paid attention because the majority of damages can be repaired and reformed by initial evaluation, consequently the spread of damage to the structures, building collapse and rising of costs can be prevented. Detection of concrete shear wall damages are designed to withstand the lateral load on the structure is critical. Since failures and malfunctions of shear walls can lead to serious damage or even progressive dilapidation of concrete structures, any change in stiffness and frequency can clearly demonstrate the occurrence of the damage. In this article, with non-linear time history analysis, the finite element model of structures with concrete shear walls subject to four earthquakes have been extracted and applying Fourier and wavelet transform, the damage of shear walls is detected. The results of displacement, base shear and hysteresis curves for experimental and numerical programs indicate a good agreement which guarantee the precision of the damage detection procedure.

Keywords Structural health monitoring · Damage detection · Concrete shear walls · Mathematical transform

1 Introduction

Over the past decades, Health monitoring of structures has been converted to an appropriate research field as a result of the growing need for the constant monitoring of large structures. Damage detection of a structure is significantly essential since early damage detection can prevent structural catastrophic damage. The term health monitoring of structures refers to the process of conducting damage detection operation in engineering structures. In this regard, any changes in material or geometric properties of a structural system that affects the system's efficiency are defined as damage. With respect to the need for health monitoring of structures, shear walls are evaluated as one of the civil structures in this article. Shear walls are designed to resist lateral loads utilized in structures.

Damage and defect in the structural performance of shear walls is reported to cause major harm or even progressive collapse of concrete structures in recent years. Many research studies have been conducted to ameliorate the accuracy and reliability of structural health monitoring methods that collect and analyze structural information automatically to determine their condition. In these methods, health monitoring of structures is based on this principal idea that the dynamic characteristics of a structure are a function of its physical characteristics. Consequently, the physical characteristic Alternation of the structure resulted from damage imposed on it can change its dynamic characteristics. Hence, structural vibration data are collected and can be utilized for detecting structural damage. The application of mathematical transforms is one of the methods to detect damage. In many cases, the effective

✉ H. Naderpour, naderpour@semnan.ac.ir | ¹Faculty of Civil Engineering, Semnan University, Semnan 3513119111, Iran.



information of the signal is hidden in its frequency content which is called signal spectrum. On the other hand, the spectrum of a signal indicates existing frequencies in the signal. With respect to this issue, a tool should be applied to measure frequency content of a signal. This tool is the same as a mathematical transform. Many researchers have worked on methods of evaluating and detecting damage in structure and studies have been conducted concerning damage detection in the shear wall.

Cawley and Adams [1] were the first ones to initiate studies in detecting damage techniques based on frequency. In this technique, damage detection will be linked to change in frequency which is occurred as a result to the alternation in mass, stiffness and other structural parameters [1]. In 2003, Melhem and Kim examined two concrete specimens under fatigue load and repetitive sudden impact and developed a damage detection in concrete structures applying Fourier and wavelet transforms with computing natural frequency before and after loading [2]. In 2005, Ge and Lui presented a method based on finite element model and using dynamic characteristics of the structure such as frequencies and modal shapes [3]. In 2009, Sasmal and Ramanjaneyulu provided a method and derived the natural frequency through transition matrix in order to detect damage its type and location. Damage detection and its location in the structure were accomplished with significant accurate [4]. In 2009, Yan et al. proposed an approach based on the use of intelligent aggregate for concrete shear wall health monitoring. Pursuant to their works, before casting shear wall, piezoelectric aggregates were placed in specified locations inside the wall and in this way an active examination network was formed to monitor the health of a shear wall specimen. The specimen underwent a cyclic loading and was gradually continued until complete damage of loading. By applying an electrical field to aggregates, a conducted stress wave was scattered from the mentioned aggregate, and other aggregates became apparent as sensors for receiving information of waves. Signals received by sensors (aggregates) were decomposed applying wavelet packet, and a dynamic index was defined based on signals' energy in different frequencies [5]. In 2011, He and Zhu surveyed vibration-based damage detection of different structures. The accurate modeling of damaged and undamaged state of structure and developing a strong algorithm are methods for vibration-based damage detection which apply the natural frequency of structures to detect damage. The exact location of damage is identified using the proposed algorithm and natural frequency with the lowest percentage of errors [6]. In 2013, Barad et al. presented a fast and effective method to determine the depth and location of

crack through an alternation in the natural frequency of structure by modeling the crack applying a coil-spring [7]. Farhidzadeh et al. investigated monitoring of failure procedure in a large scale reinforced concrete shear wall. A shear wall laboratory specimen underwent cyclic loading with displacement control, and wall cracking behavior was evaluated simultaneously by continuous analysis of acoustic waves' emission as a result of the material fracture or the plastic deformation occurrence, the wall cracking behavior was evaluated [8]. In 2013, Vafaei et al. proposed a method for straight off identification of seismic damage utilizing an artificial neural network. Inter-story drift and plastic hinge rotation of concrete shear walls are contemplated as the input and output of MLP neural network respectively. A 5 story building is applied to exhibit the power and efficiency of the presented method. 9 different recorded earthquakes are considered for this study. In all cases, except in 4 cases, the network has performed shear wall damage detection properly [9]. In addition, soft computing approaches such as artificial neural networks (ANN), Group Method of Data Handling (GMDH), and Gene Expression Programming (GEP) were successfully implemented by different researchers in the context of civil and structural engineering [10–19]. In 2014, Khiem and Toan presented a new method to detect an unspecified number of cracks in the structure by contemplating non-linear terms associated with crack intensity using natural frequency calculation [20]. In 2015, Lin demonstrate how bending cracks alternate vibration properties like frequency response function and the way these properties can be utilized to detect damage [21]. In 2016, Damage identification based on Peak Picking Method and Wavelet Packet Transform for structural equation has been used by Naderpour and Fakharian [22]. In 2017, a model-free output-only wavelet-based damage detection analysis was performed in order to achieve perturbation of detailed function of acceleration response in bridge piers [23]. It is worth to be noted that the safety measures of buildings in terms of structural reliability and probabilistic point of view were studied in different researches. However, this perspective of analysis was not considered in the current study [24–29].

2 Research significance

In this study, the crack is modeled like a coil-spring, and vibration properties such as natural frequency and mode shape are calculated and used to detect damage. The purpose of this article is to apply Fourier and wavelet transform to detect damage and identify the time of damage in

shear wall respectively. In order to do that, the structural finite element model is created in SeismoStruct software and is subjected to nonlinear time history analysis by four earthquakes. Subsequently the natural frequency is derived using Fourier transform and damage occurrence becomes apparent and the time of damage occurrence will be identified applying wavelet transform eventually.

3 Methodology

The intention of applying a mathematical transform on a signal is to obtain additional information that is not reachable in the first raw signal. In many cases, signal beneficial information is hidden in its frequency content called signal spectrum. In a simpler way, the spectrum of a signal is as a representative of its frequencies. A tool is needed in order to examine the frequency content of a signal. This tool is the same Fourier transform which is described in the following section. According to Fig. 1 the Fourier transform partitions a signal to a set of infinite exponential function in which each of them contains different frequencies. The Fourier transform of a continuous signal in time is computed by the Eq. (1).

$$X(f) = \int_{-\infty}^{+\infty} x(t)e^{-j2\pi ft} dt \tag{1}$$

where t is time and f is frequency. Relation (1) indicates signal Fourier transform $x(t)$. In relation (1), it can be observed that $x(t)$ signal is multiplied by an exponential term with the specified frequency, f , and then it is integrated on all time intervals. It should be noted that exponential term can be written as Eq. (2):

$$e^{j2\pi ft} = \cos(j2\pi ft) + j \sin(j2\pi ft) \tag{2}$$

The aforesaid expression contains a real cosine term with f frequency and an imaginary sinus term with f frequency. Consequently, multiplying the time signal by a complex

exponential function which is, in fact, the combination of two periodic functions with f frequency is accomplished in Fourier transform. In the next step, this multiplication is integrated. On the other hand, all points of this multiplication are added together. Lastly, if the result of this integration (which is a type of infinite summation) is a big number, it can be concluded that that $x(t)$ signal merely a frequency component highlighted in f frequency. If the outcome is a small number, it can be said that f frequency is component is not dominant in this signal. When the outcome of integral is derived zero, it indicates the absence of such frequency in the signal as well. The Fourier transform only displays that whether f frequency does exist in the described signal or not, but gives no information about the time interval corresponding to the visibility of frequency. The wavelet transform of a function analysis is based on wavelet functions. Wavelets are transformed and scaled samples of a function (mother wavelet) with finite and strongly damped oscillating length. The wavelet transform, as shown in Fig. 2, is conducted on different time sections of signal separately, and the width of the window is alternated along frequency component change which is the most important feature of wavelet transform indeed.

$$CWT_x^\psi = \Psi_x^\psi(\tau, s) = \frac{1}{\sqrt{|s|}} \int_{-\infty}^{+\infty} x(t)\psi^*\left(\frac{t-\tau}{s}\right) dt \tag{3}$$

where τ and S are transmission and scale parameters respectively. The concept of transmission determines window displacement value and clearly contains time information of the transform.

4 Modeling

The utilized program was SeismoStruct which is a Finite Element software having the ability to predict the behavior of structures subjected to static/dynamic loadings which considers both geometric nonlinearities and inelasticity of materials.

Cantilever web wall, a flange wall, a pre-cast segmental pier and gravity columns are the elements of the structure. At each floor, the slab is simply supported by the wall and the columns.

The walls were modelled using 3D force-based inelastic frame elements having 4 integration sections. Furthermore, 200 fibers were used in section equilibrium computations. The columns were modelled in terms of truss elements. The precast column was modelled using an elastic frame element with the following properties:

$$EA = 3.9720 \times 10^9 \text{ (lb);}$$

$$EI \text{ (axis2)} = 3.3035 \times 10^{12} \text{ (lb-in}^2\text{);}$$

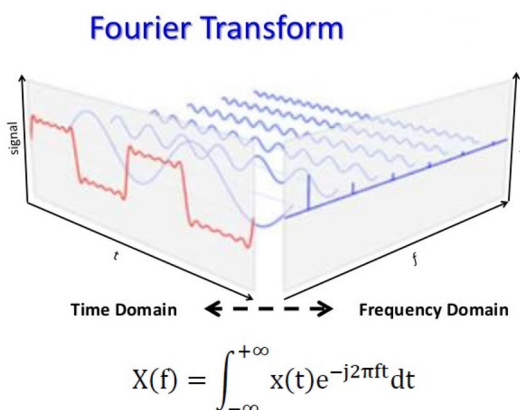


Fig. 1 Fourier transform

Fig. 2 Wavelet transform

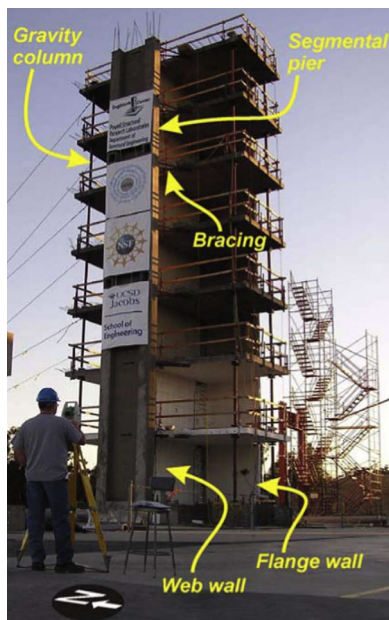
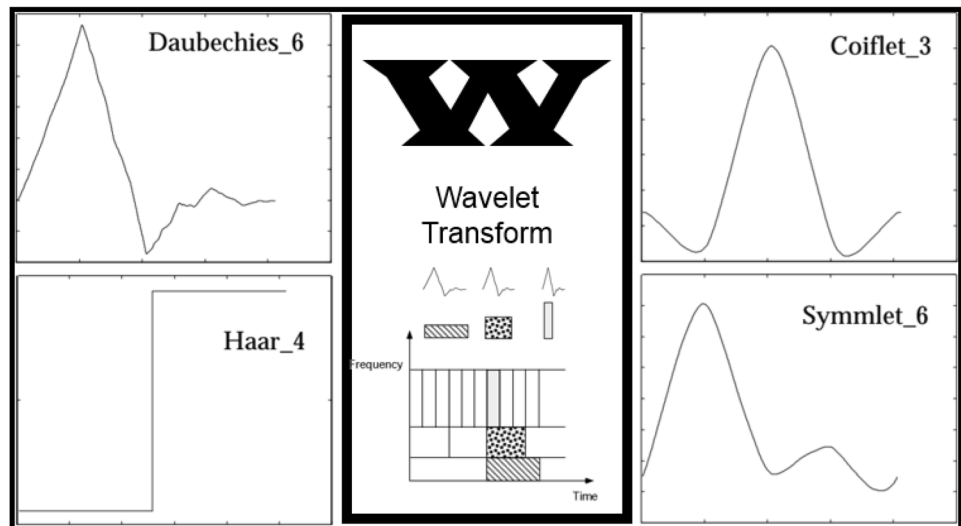


Fig. 3 An overview of experimental program details [30]

$$EI \text{ (axis3)} = 1.7548 \times 10^{11} \text{ (lb-in}^2\text{);}$$

$$GJ = 5.7887 \times 10^{10} \text{ (lb-in}^2\text{)}.$$

Modeling of a seven story building with the full-scale rectangular shear wall, Fig. 3, that is undergone shaking table test of the network for earthquake engineering simulation in the university of California at San diego (2006) by four earthquakes is discussed through SeismoStruct in this section [30].

Figures 4 and 5 present plan view of the test structure, web wall instrumentation and wall reinforcement.

According to Fig. 6, four real earthquakes are simultaneously applied in a way which is separated from each other by a low-domain noise, and are used in a way that the first earthquake EQ1 is with low-intensity and the next two earthquakes, EQ2 and EQ3, are with medium intensity and the last earthquake, EQ4, is with high intensity. The use of four earthquakes input motions with distinct features and intensities allowed monitoring of the development of different damage states in the building specimen. Overall, the response was slightly nonlinear for EQ1, moderately nonlinear for the “medium” intensity input motions EQ2 and EQ3, and highly nonlinear for input motion EQ4. During test EQ1, limited yielding occurred in the longitudinal reinforcing steel of the web wall. After this test, cracking of the web wall was widespread and visible up to the fourth floor. During tests EQ2 and EQ3, moderate yielding occurred in the web wall longitudinal reinforcement. Finally, during test EQ4, localized plasticity developed at the first floor of the web wall. Details of these earthquakes are presented in Table 1.

With respect to laboratory work, the modeling is accomplished by dimension and properties of the main structure. Finite element model of test structure in SeismoStruct is shown in Fig. 7.

The used earthquake associated with white noise, Fig. 8, which is applied in the program is depicted in Fig. 9.

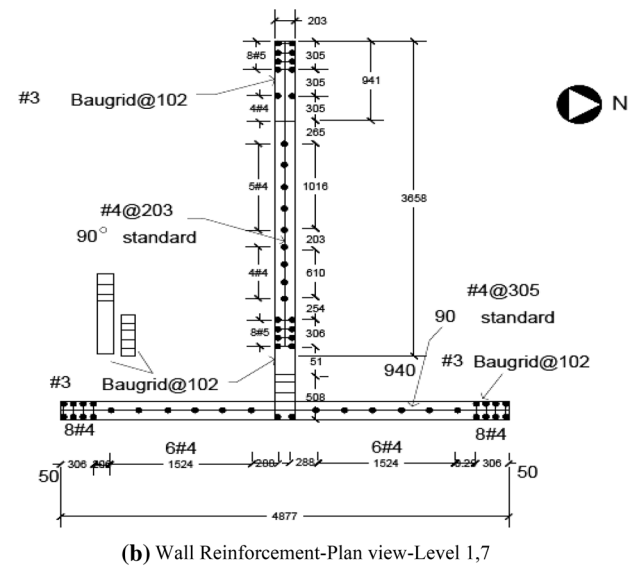
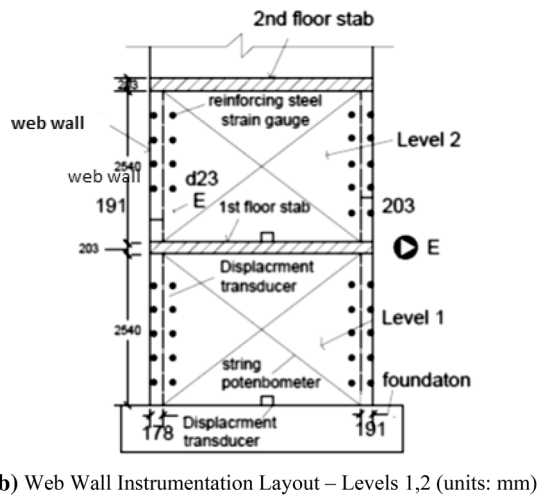
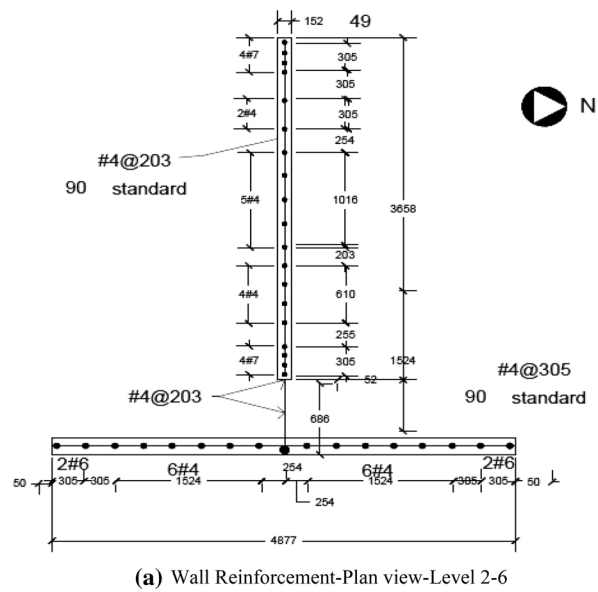
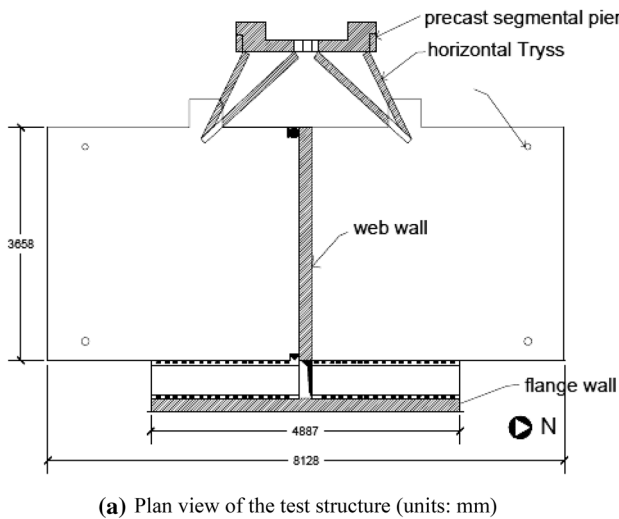


Fig. 4 Test structure geometry [30]

Fig. 5 Test structure—plan view of reinforcement (units: mm) [30]

5 Verification

In order to apply the created model in SeismoStruct software, proper accordance is required to be obtained between test results and the created model.

According to Figs. 10, 11, 12, and 13, experimental versus analytical results—top displacement—time for (EQ1), (EQ2), (EQ3), (EQ4), experimental versus analytical results—base shear—time (EQ4) in Fig. 14 and experimental versus analytical results—system base shear force—roof lateral relative displacement in Fig. 15, results of the modeled structure and real tested model varies in some cases,

and they are proximate in many cases particularly the forth earthquake.

As shown, the results of the structural model and the actual model tested at the University of San Diego in some cases, such as displacement under the fourth earthquake, are very close and in some cases divergent. This discrepancy can be due to the small differences in inputs to software over actual values and the possibility of modeling except for actual structures. In addition, laboratory work has a small percentage of errors, which can be exacerbated

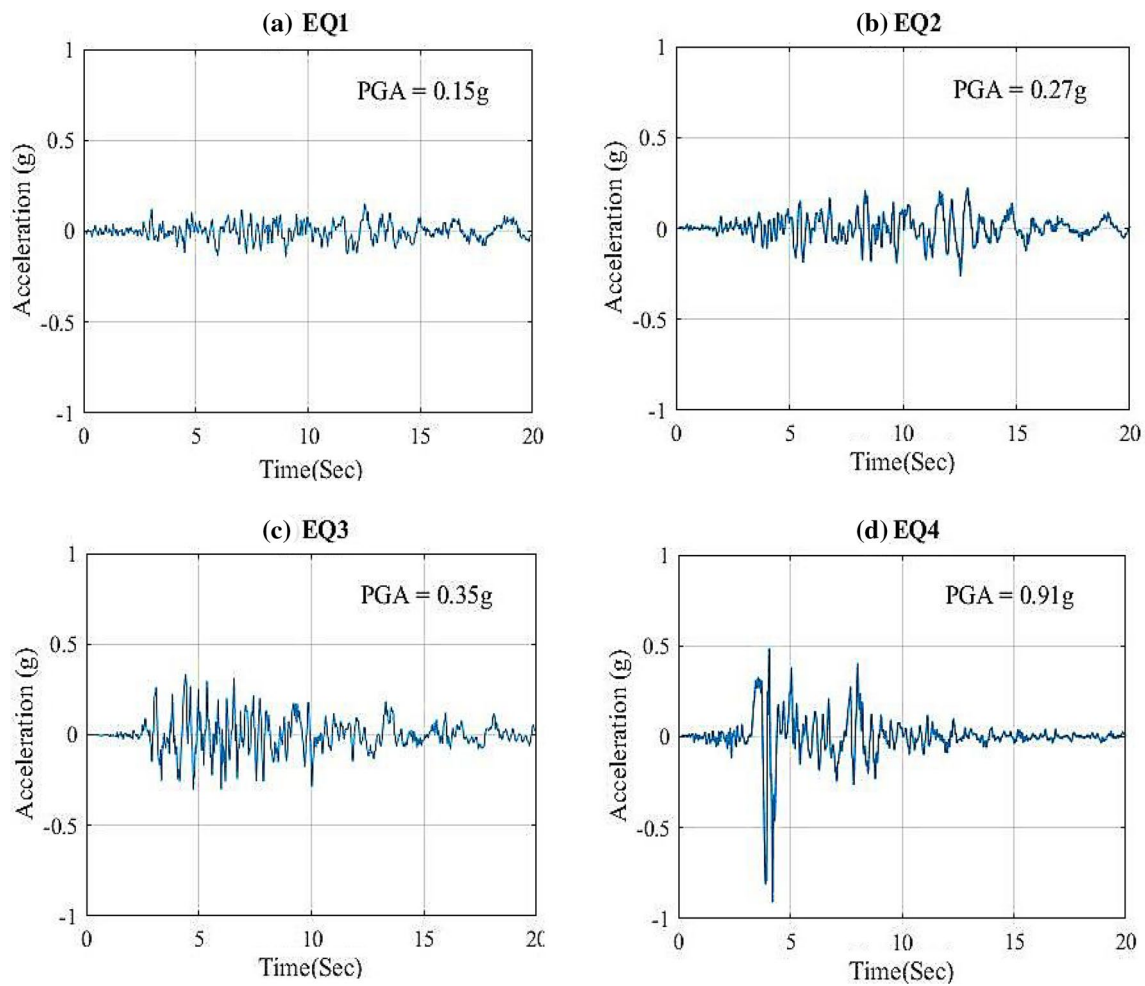


Fig. 6 Earthquake ground acceleration time histories applied to the test structure [30]

Table 1 Ground motions: general information [30]

EQ	Earthquake record	Station	Year of occurrence	PGA (g)
EQ1	San Fernando	Van Nuys (long. Comp)	1971	0.15
EQ2	San Fernando	Van Nuys (transv. Comp)	1971	0.27
EQ3	Northridge	Oxnard Boulevard Woodland Hill	1994	0.35
EQ4	Northridge	Sylmar Olive View Medical Center	1994	0.91

by a low percentage of comparison with model results. But the overall results of the software allow us to use the built model to continue the work of identifying damage, especially under an earthquake that causes the most damage to the structure, which is the main purpose of damage detection.

6 Damage detection

In this section, structural acceleration response under 4 earthquakes is contemplated as SeismoStruct software output and is applied to identify damage in the structure. In order to detect damage before applying wavelet transform to structural acceleration responses, at first, the

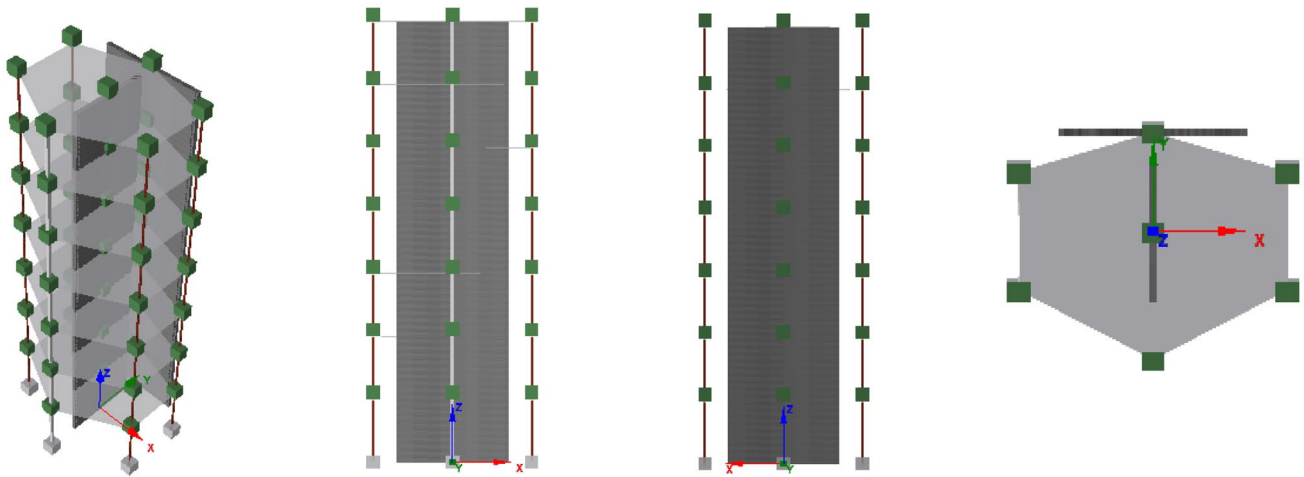


Fig. 7 Finite element model of test structure in SeismoStruct

Fig. 8 The first 50 s of the banded white noise base acceleration time history applied to the test structure

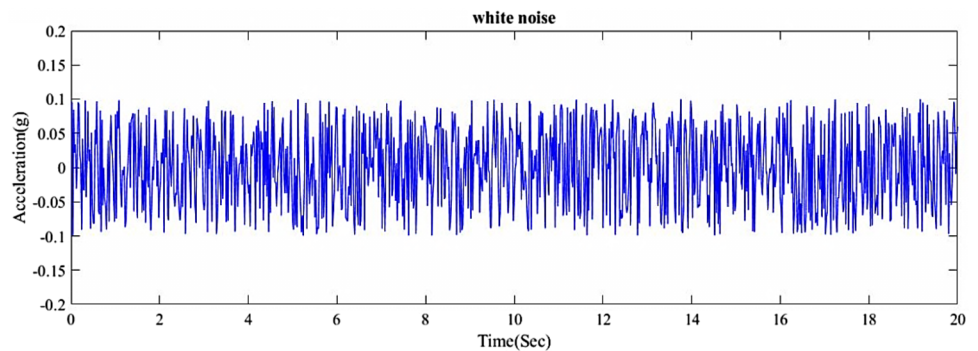
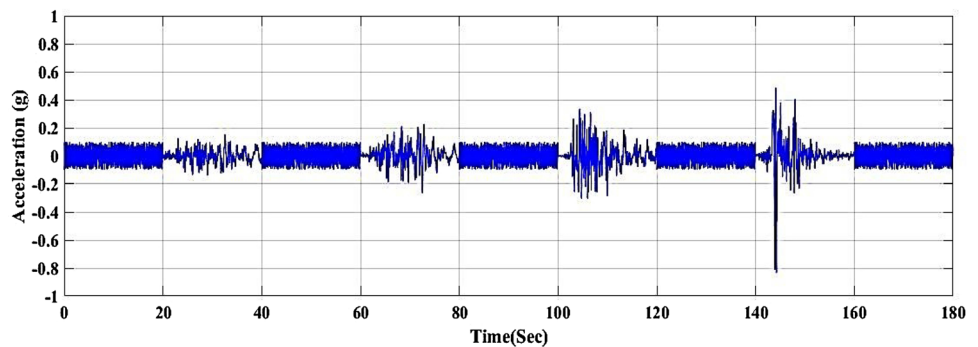


Fig. 9 Input ground motions



structural response frequency is derived from vibration response under white noise before and after each of earthquakes by Fourier transform through SeismoStruct software over all walls which the results for specimens on the walls of all seven floors are illustrated. An example of these results is depicted in Fig. 16, and due to the limitation of space, the other results are presented in the “Appendix”.

Fourier spectrum of acceleration response based on applied white noises before and after each record is examined which are illustrated in Figs. 17, and 30, 31, 32, 33, 34, 35 of the “Appendix”.

As shown in Fig. 18 frequency change value at the beginning of loading and in the first earthquake is high, and in the next two earthquakes contains no sensible

Fig. 10 Experimental versus analytical results—top displacement–time (EQ1)

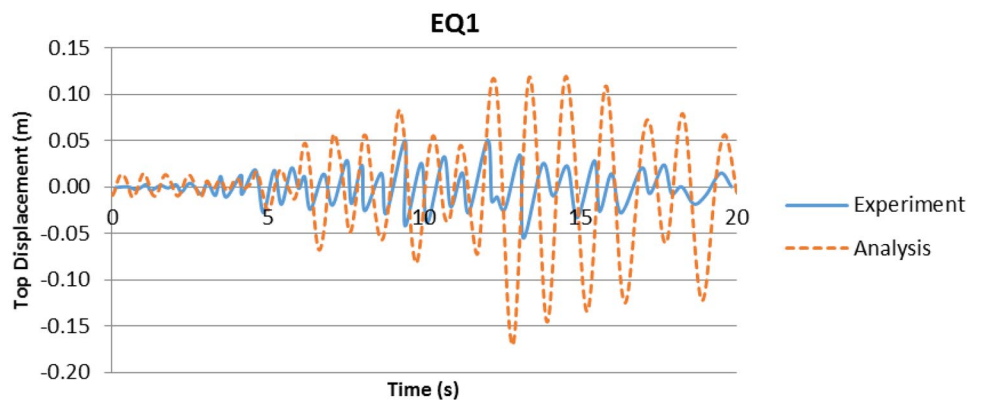


Fig. 11 Experimental versus analytical results—top displacement–time (EQ2)

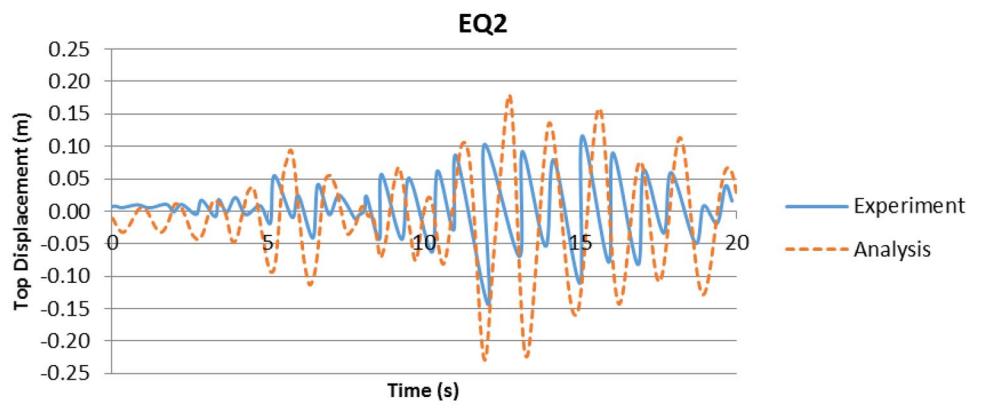
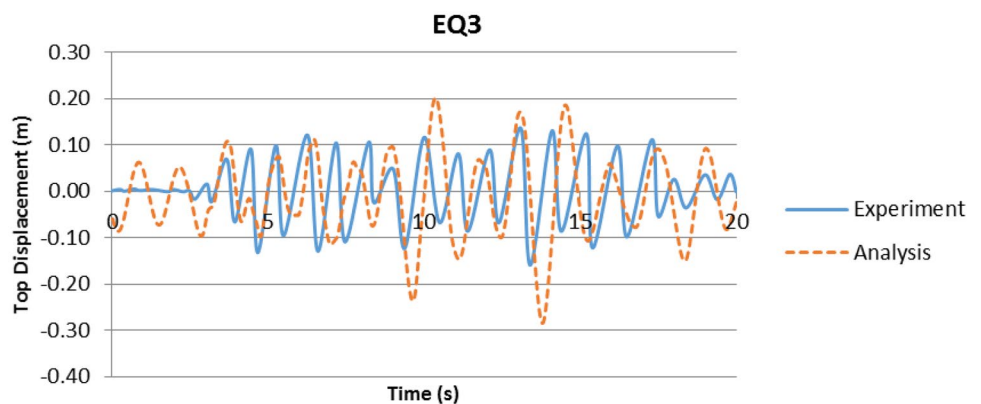


Fig. 12 Experimental versus analytical results—top displacement–time (EQ3)



change and structural stiffness faces significant reduction due to healthy structure and slight damage like concrete cracking at the beginning of the analysis.

However, the energy of structure is dissipated due to reinforcement yielding, and structural nonlinear behavior and its impact on damage development and stiffness change are reduced in the end. The structural acceleration

Fig. 13 Experimental versus analytical results—top displacement–time (EQ4)

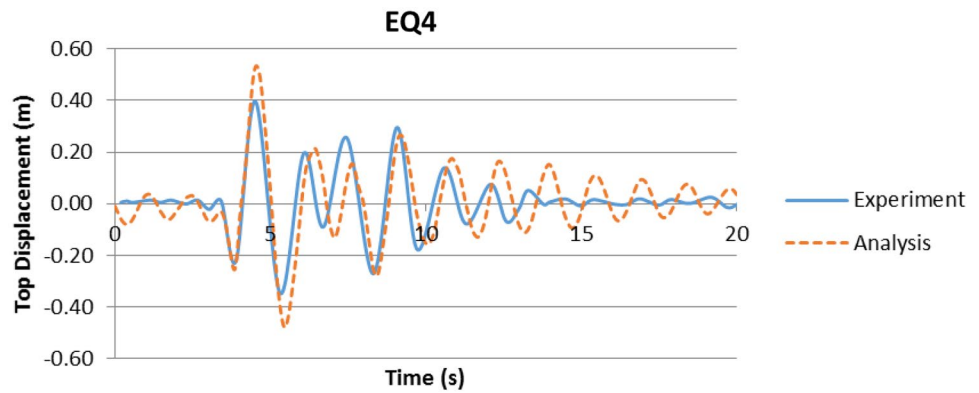


Fig. 14 Experimental versus analytical results—base shear–time (EQ4)

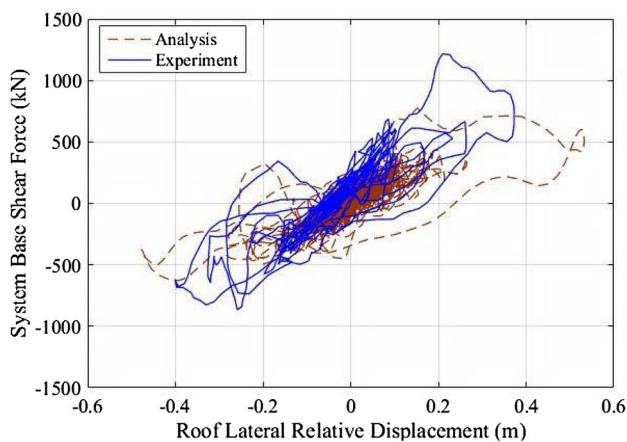
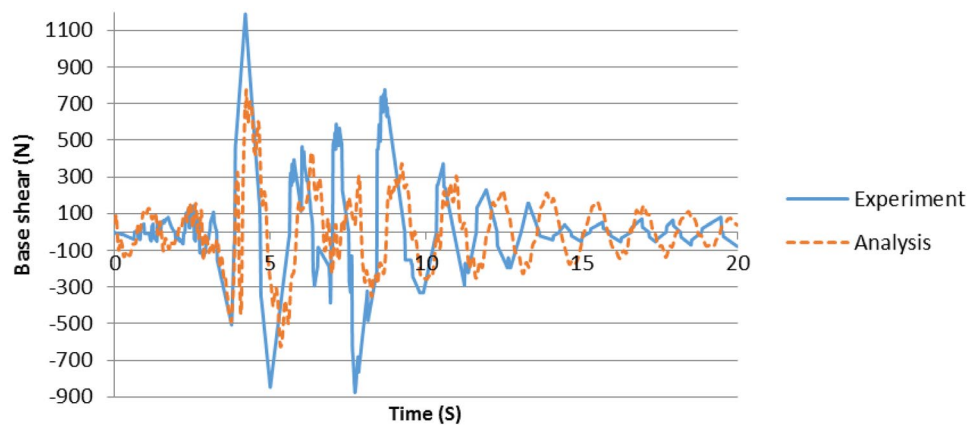


Fig. 15 Experimental versus base shear–time system base shear force–roof lateral relative displacement

response is evaluated by wavelet transform. Diagrams are presented in the following figures.

As can be observed from Figs. 19, 20, 21, and 22, the details indicate damage in the structure. The summary is illustrated in Fig. 23.

According to time of damage in shear walls for each record, Fig. 23, the effective time of the second and the fourth earthquake is the same as in all seven stories. The time of damage within next earthquakes occurrence is reduced as a result to an increase in earthquake intensity and also developing earthquake induced damage. But in the first earthquake, the effective time of damage in the first to the third story is half of the effective time in stories 4–7. This reduction is due to applying earthquake to a healthy structure and with respect to the small value of earthquake decreased frequency reduction is only as a representative for small damages and the real effective time of damages will become apparent over time.

The effective time is scaled based on the first earthquake in Table 2.

As can be seen from the first earthquake and when the second earthquake enters, the time of damage is reduced. But by the time of the second earthquake the time was reduced to half of the first state and by the fourth earthquake this time get to one third. This downward trend is justified by the reasons given.

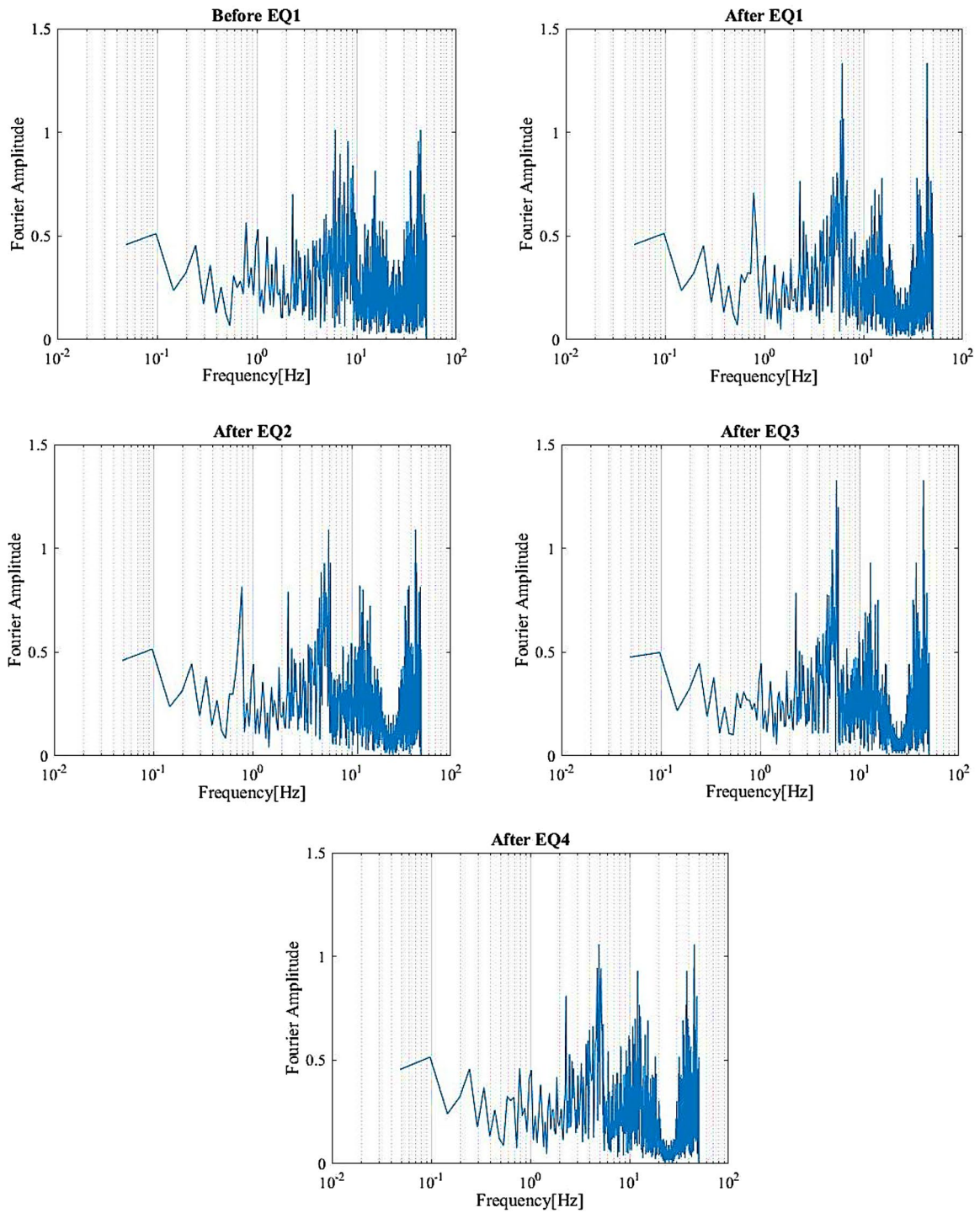


Fig. 16 Fourier spectrum before and after earthquake—first level

Fig. 17 Fourier spectrum before first and after last earthquake—first level

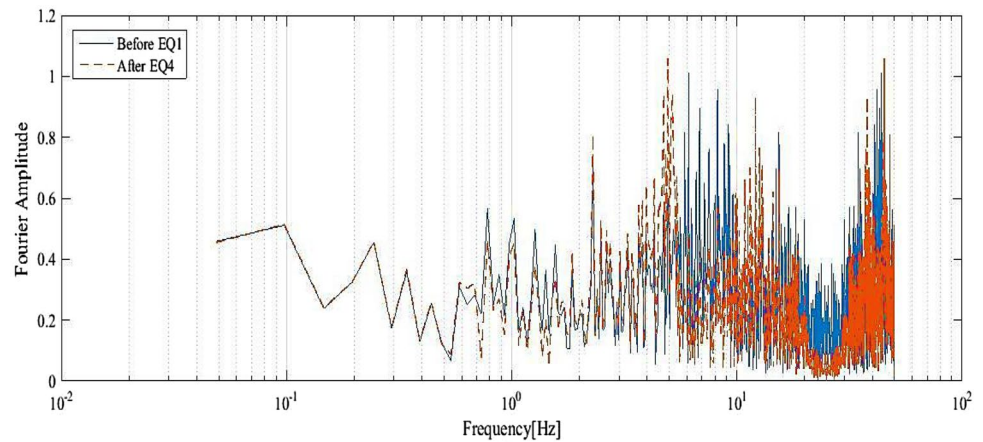
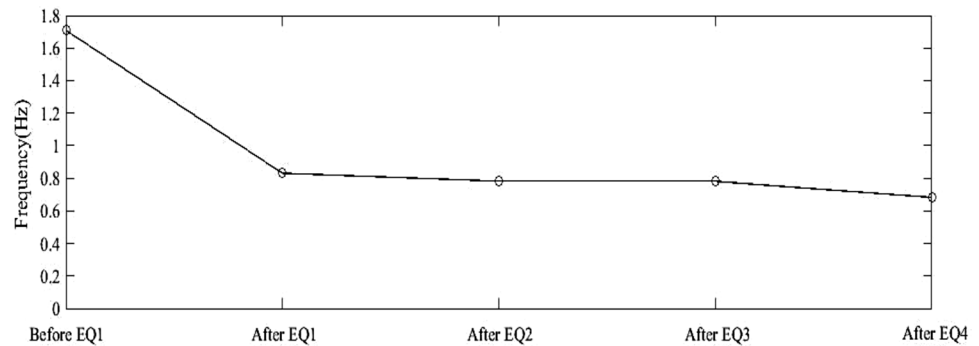


Fig. 18 Vibration frequency history during analysis



7 Conclusion

Health monitoring of structures and damage detection are the ability to exhibit structural performance and evaluation of any damage in the early stages in order to reduce structural maintenance cost and enhance safety and reliability of structure. Health monitoring of structure is essential since it's required for sustaining safety of structures and providing occupants' safety. The nonlinear time history analysis was accomplished on the 7 story model structure having a shear wall. In this article, at first 4 earthquakes with different PGA with a white noise were applied to the model structure after each earthquake. The results consisted of structural response due to the recorded earthquake and white noise.

- The Fourier transform was applied to white noise response. The result demonstrates the damage fre-

quency reduction due to stiffness reduction. Subsequently, the time of damage can be obtained by applying a wavelet transform on structural acceleration response caused by 4 earthquakes. It can be concluded from the results that signal processing is a strong technique for structural health monitoring.

- The result of displacement, base shear and hysteresis curves due to experimental and numerical programs display a good agreement.
- The alternations in stiffness and frequency of structures in both experimental and numerical models during four earthquake records reveal a good agreement.
- By direct comparison of the results for undamaged and damaged structures, one cannot detect the possible damages for shear walls while in terms of signal decomposition due to structural deformation using wavelet analysis, the damages could be detected as spikes of decomposed curves.

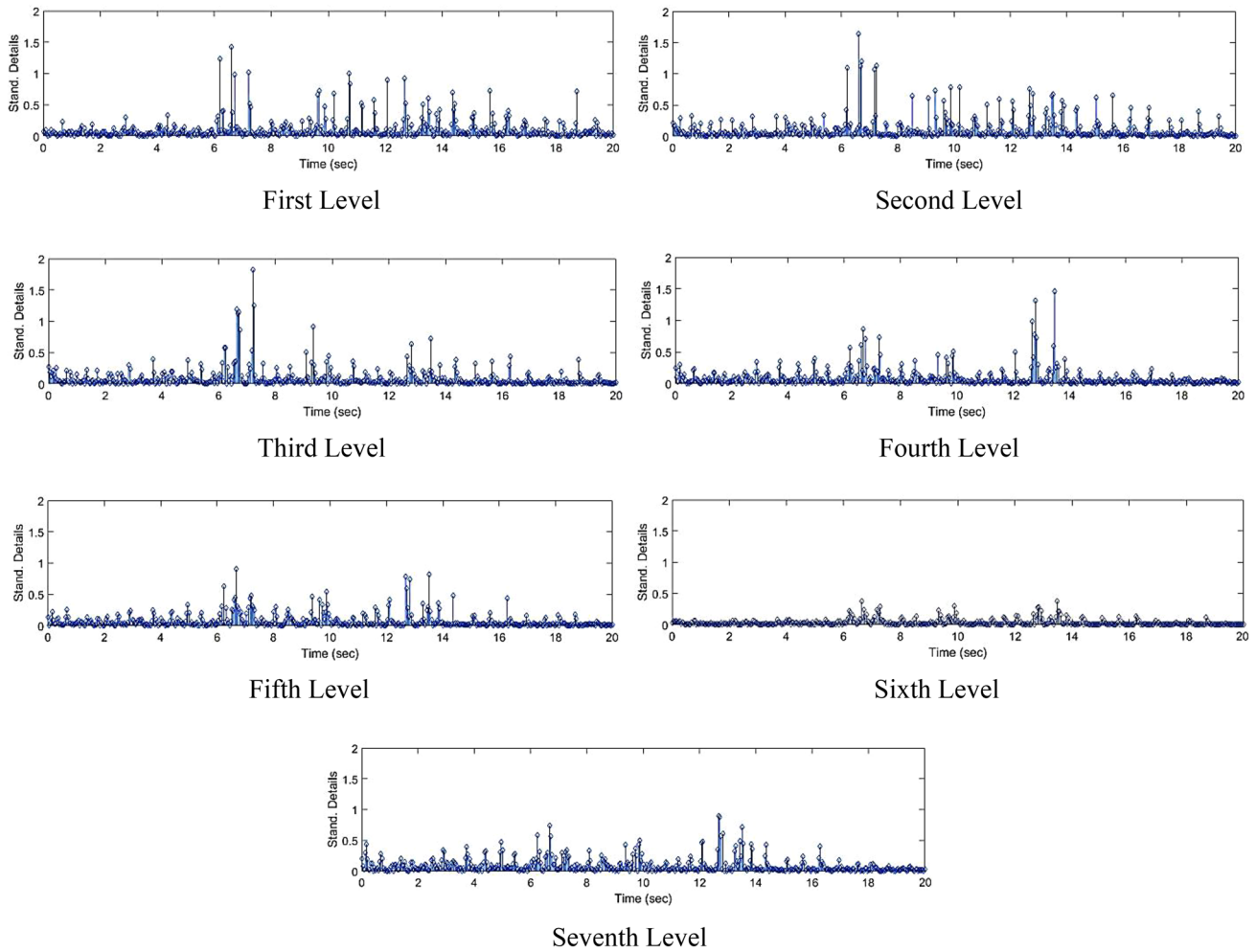


Fig. 19 Standardized decomposed details of acceleration from EQ1

- In order to determine the time of damage occurrence, it is required to derive the structural response of one node of a model subject to earthquake record. Then, by applying discrete wavelet transformation and decomposing the acceleration signal and investigation of standardized details of response, the time of damage could be approximated.
- The results indicate that the time of damage in next records has better precision when compared to that of first earthquake record.

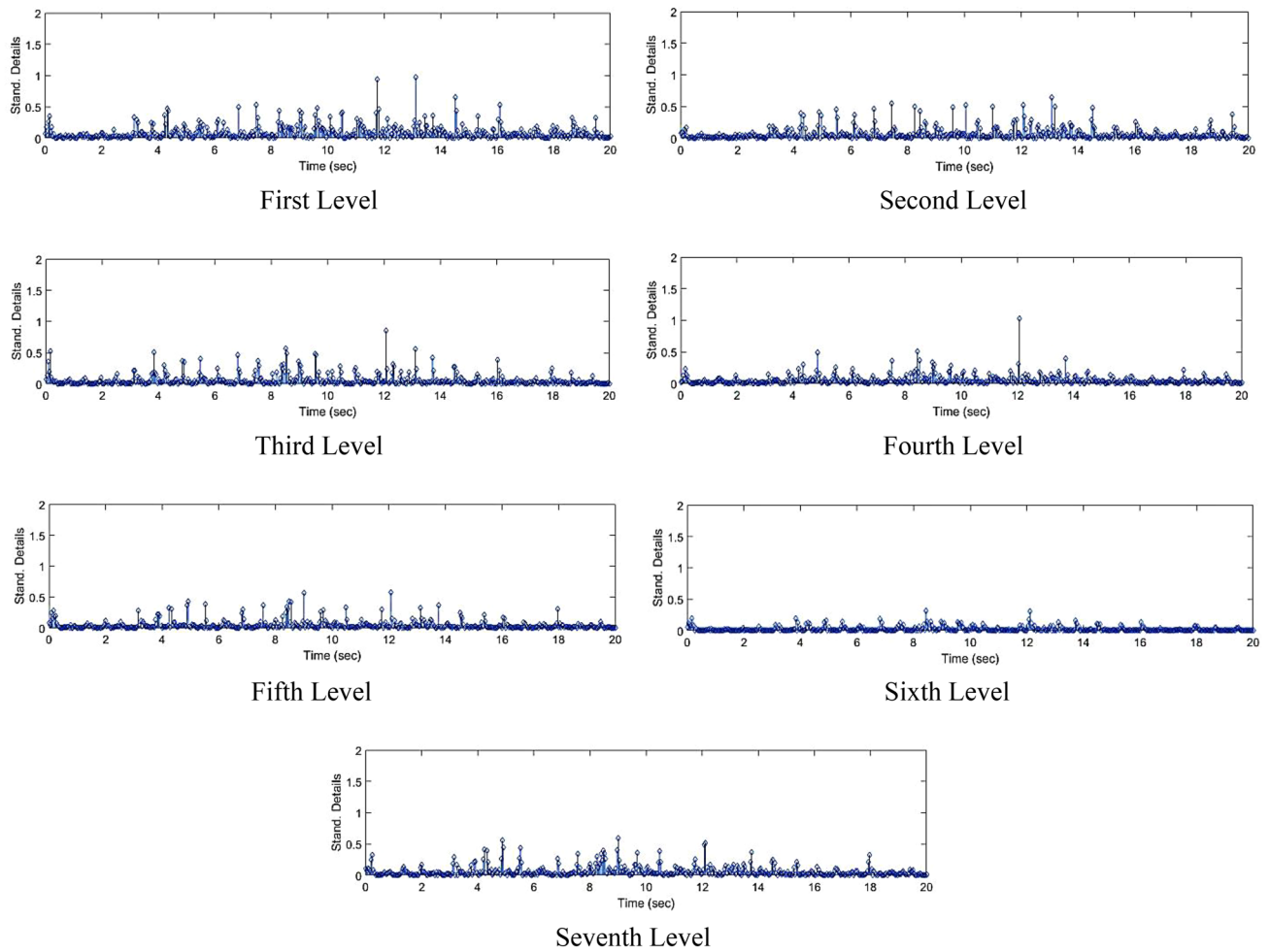


Fig. 20 Standardized decomposed details of acceleration from EQ2

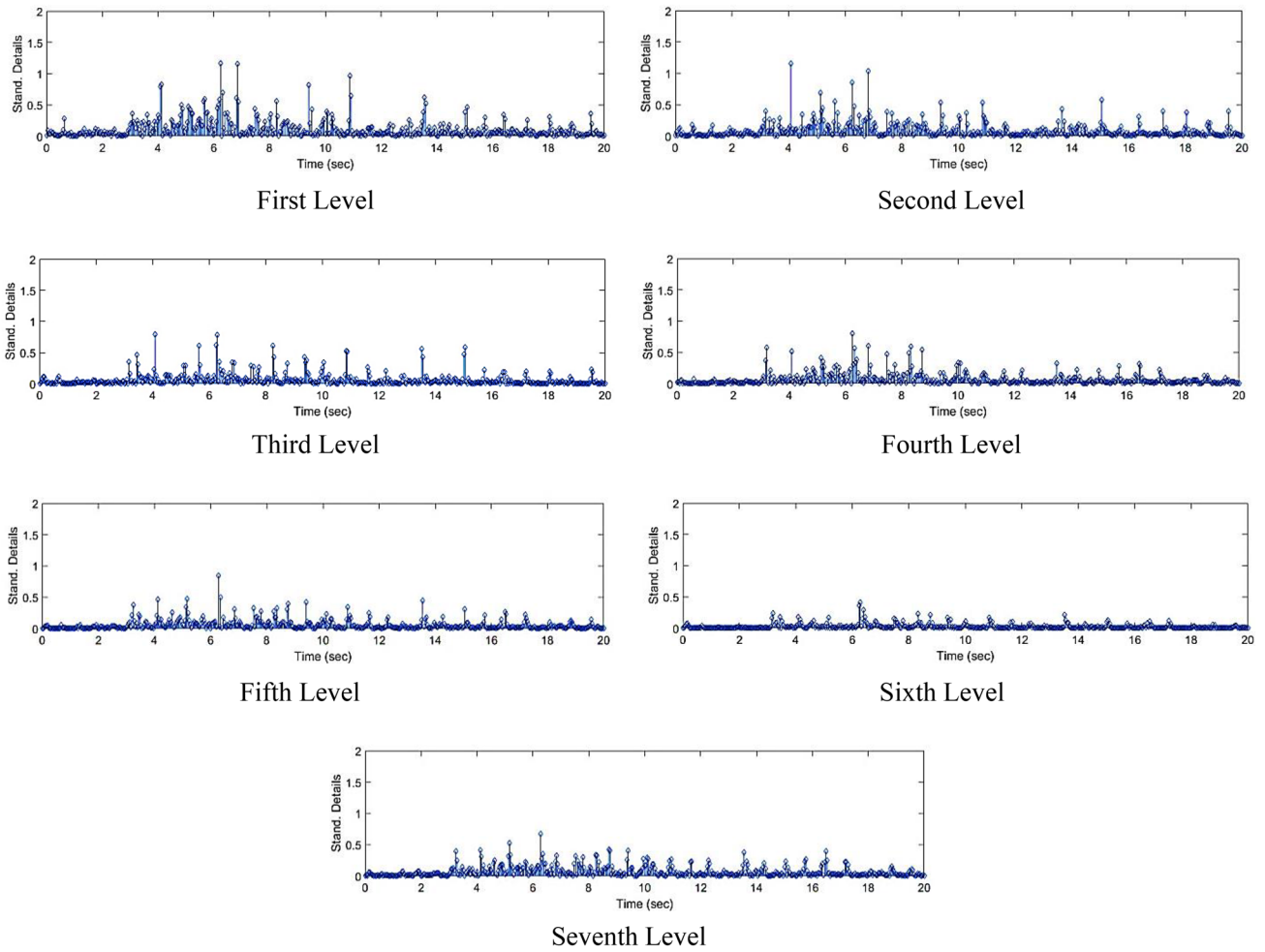


Fig. 21 Standardized decomposed details of acceleration from EQ3

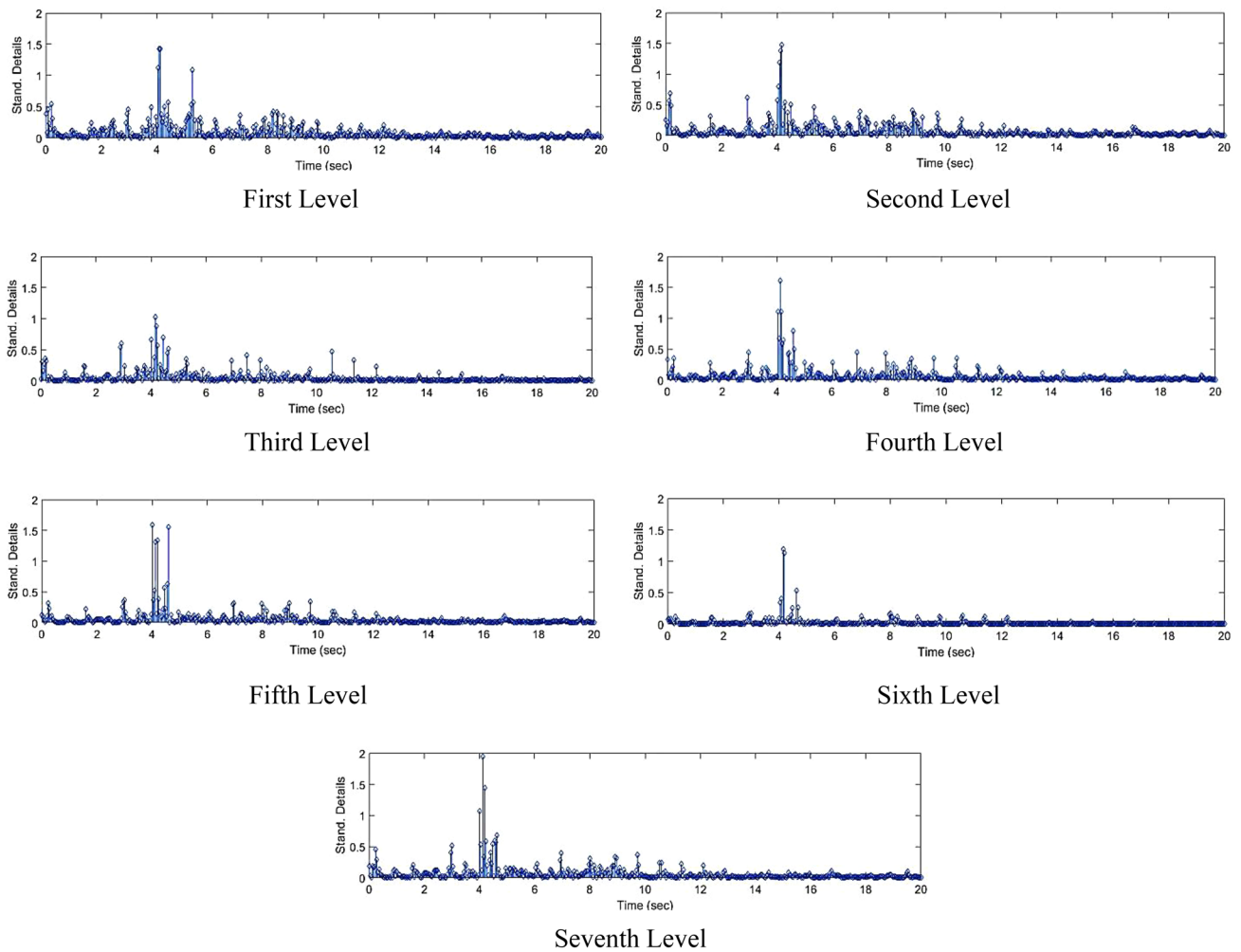


Fig. 22 Standardized decomposed details of acceleration from EQ4

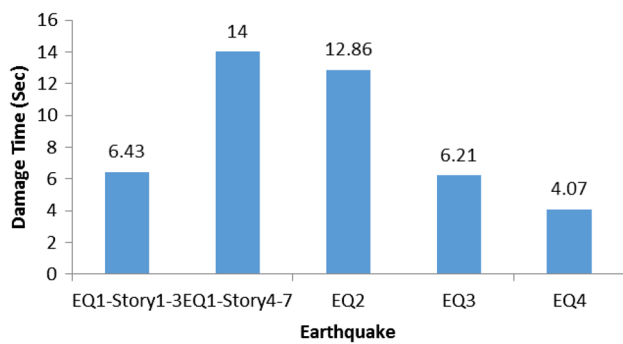


Fig. 23 Time of damage in shear walls for each record

Table 2 Time of damage

EQ	Time of damage	t_{EQ4}/t_i
EQ1	1	14
EQ2	0.92	12.86
EQ3	0.44	6.21
EQ4	0.29	4.07

Compliance with ethical standards

Conflict of interest The authors confirm that there is no conflict of interests.

Appendix

The representative results of this numerical study is depicted in Figs. 24, 25, 26, 27, 28, 29, 30, 31, 32, 33, 34, and 35.

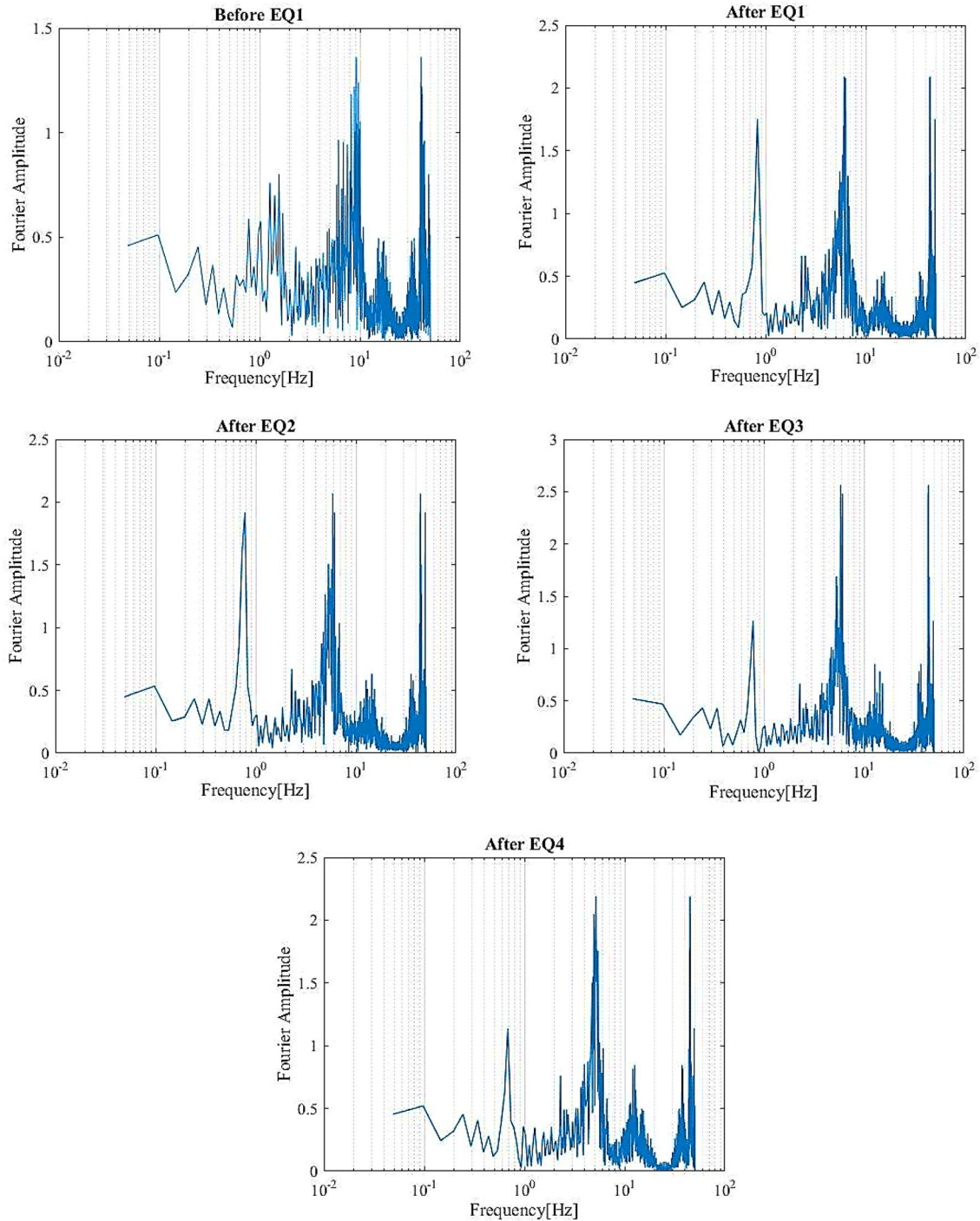


Fig. 24 Fourier spectrum before and after earthquake—second level

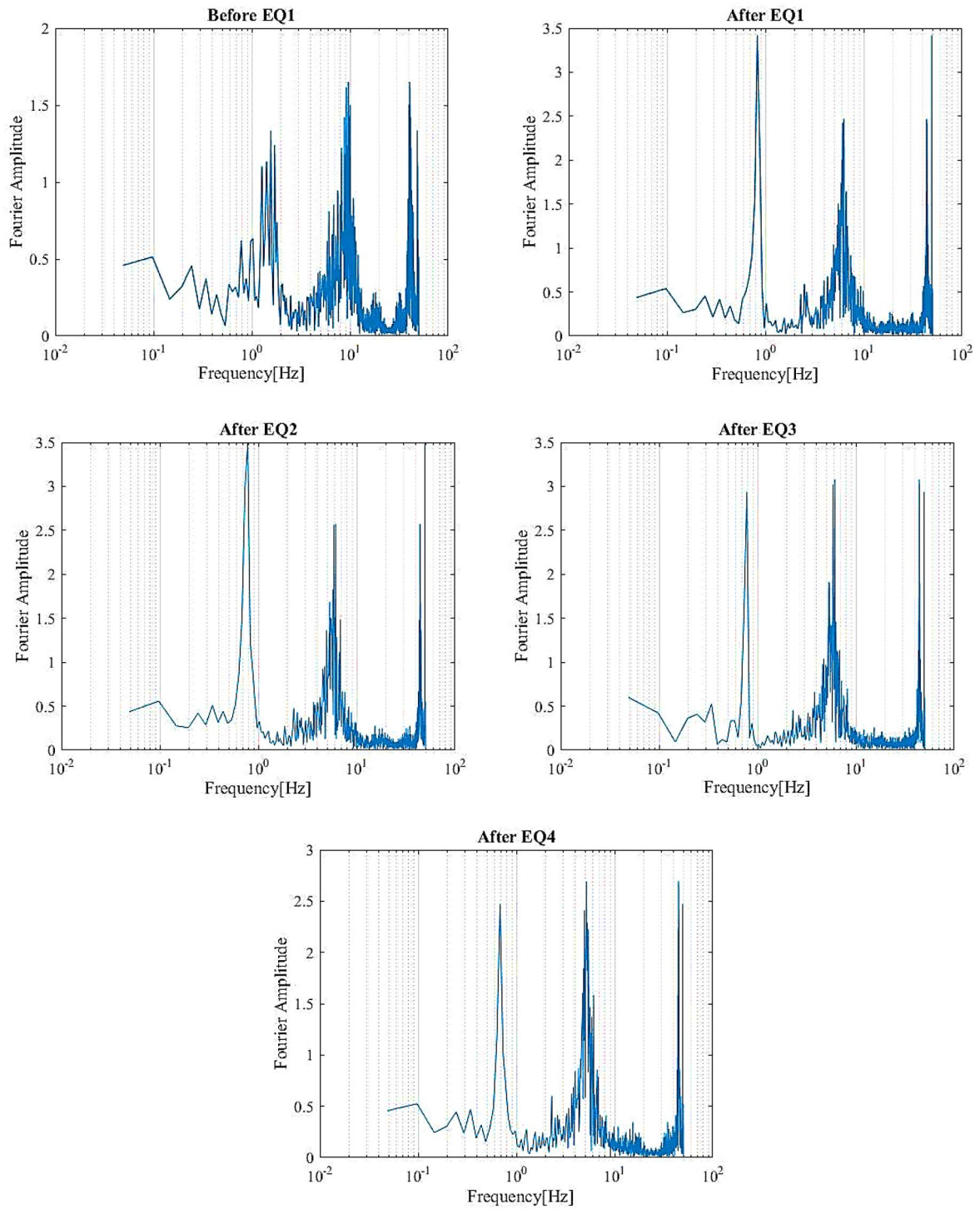


Fig. 25 Fourier spectrum before and after the earthquake—third level

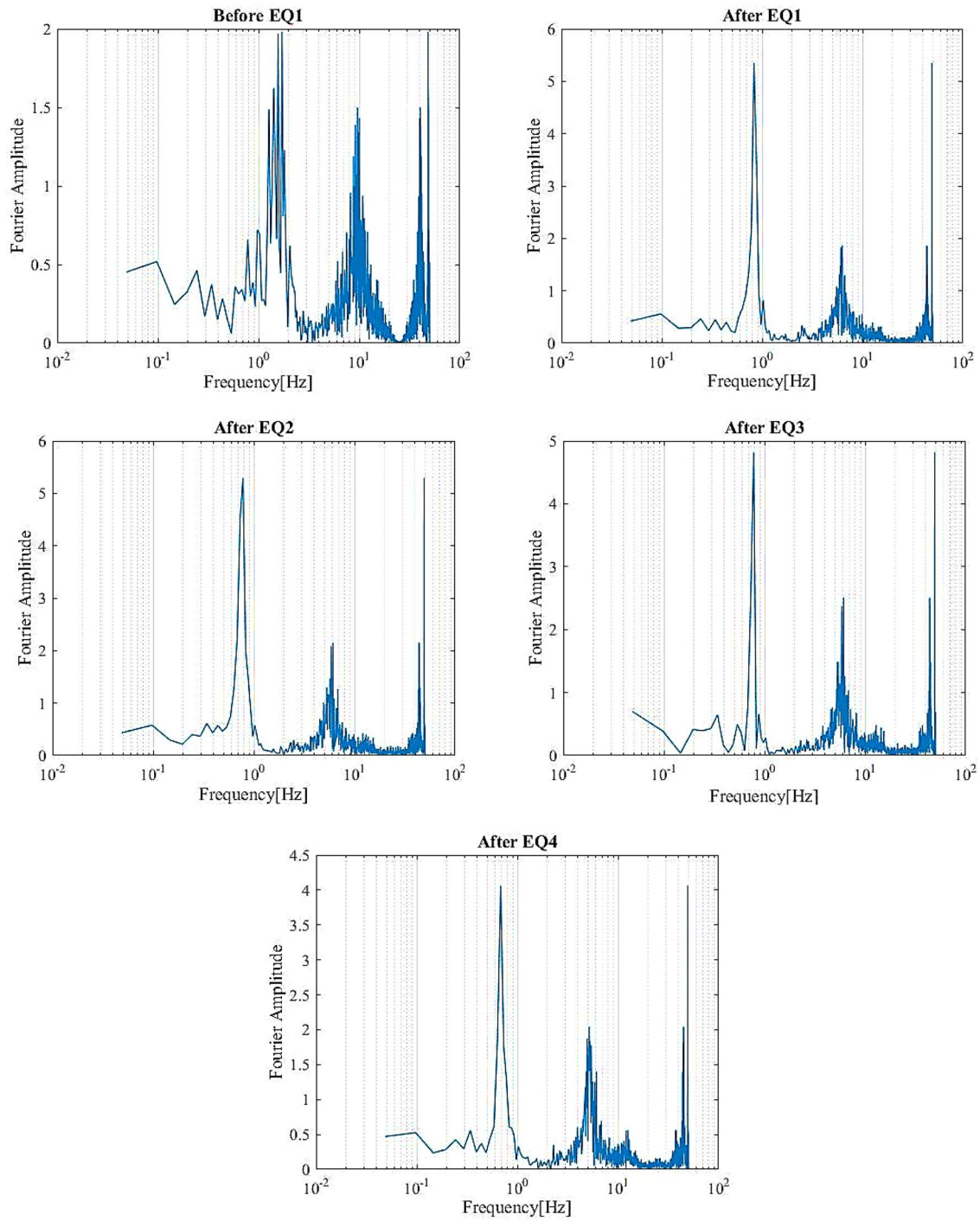


Fig. 26 Fourier spectrum before and after the earthquake—fourth level

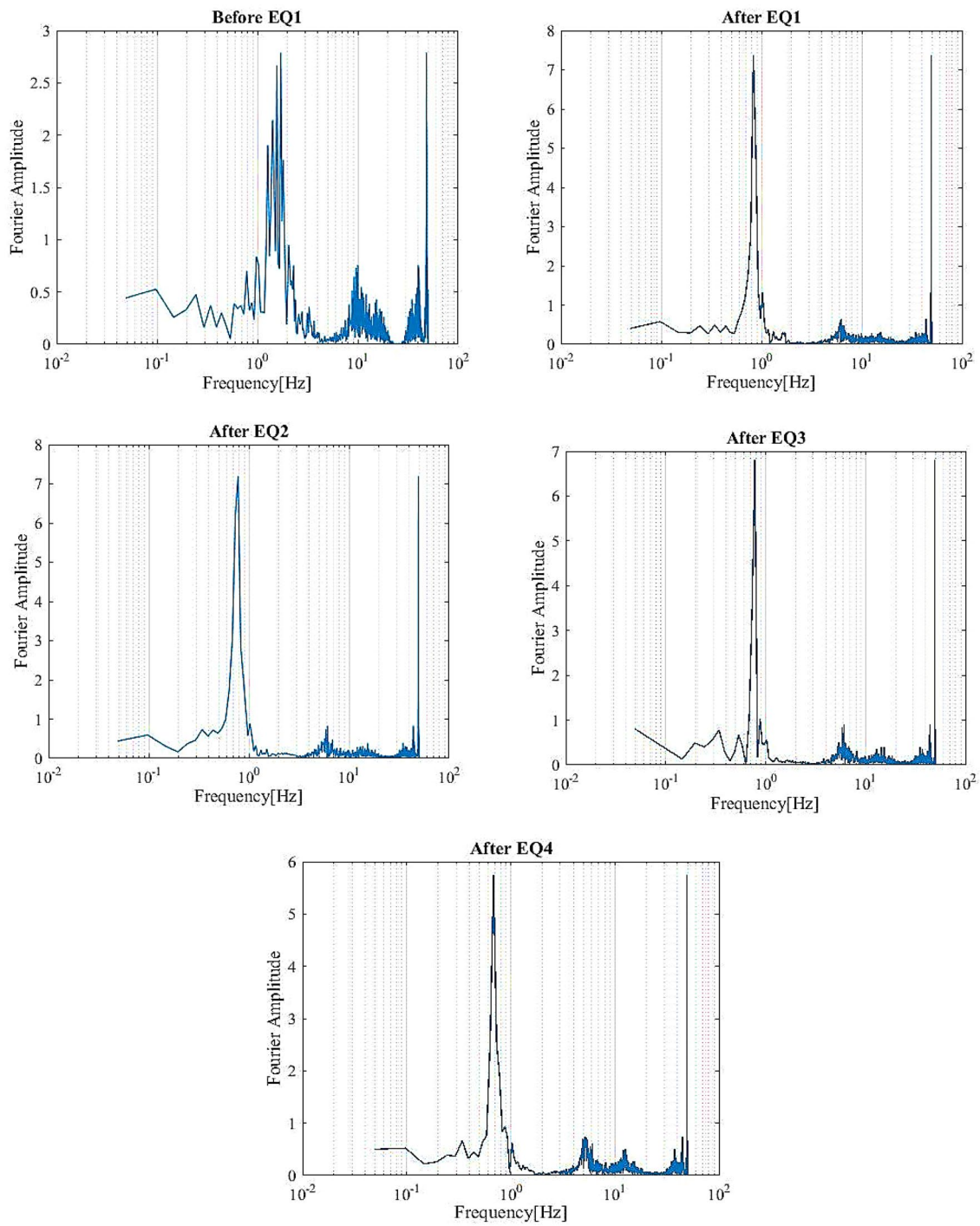


Fig. 27 Fourier spectrum before and after the earthquake—fifth level

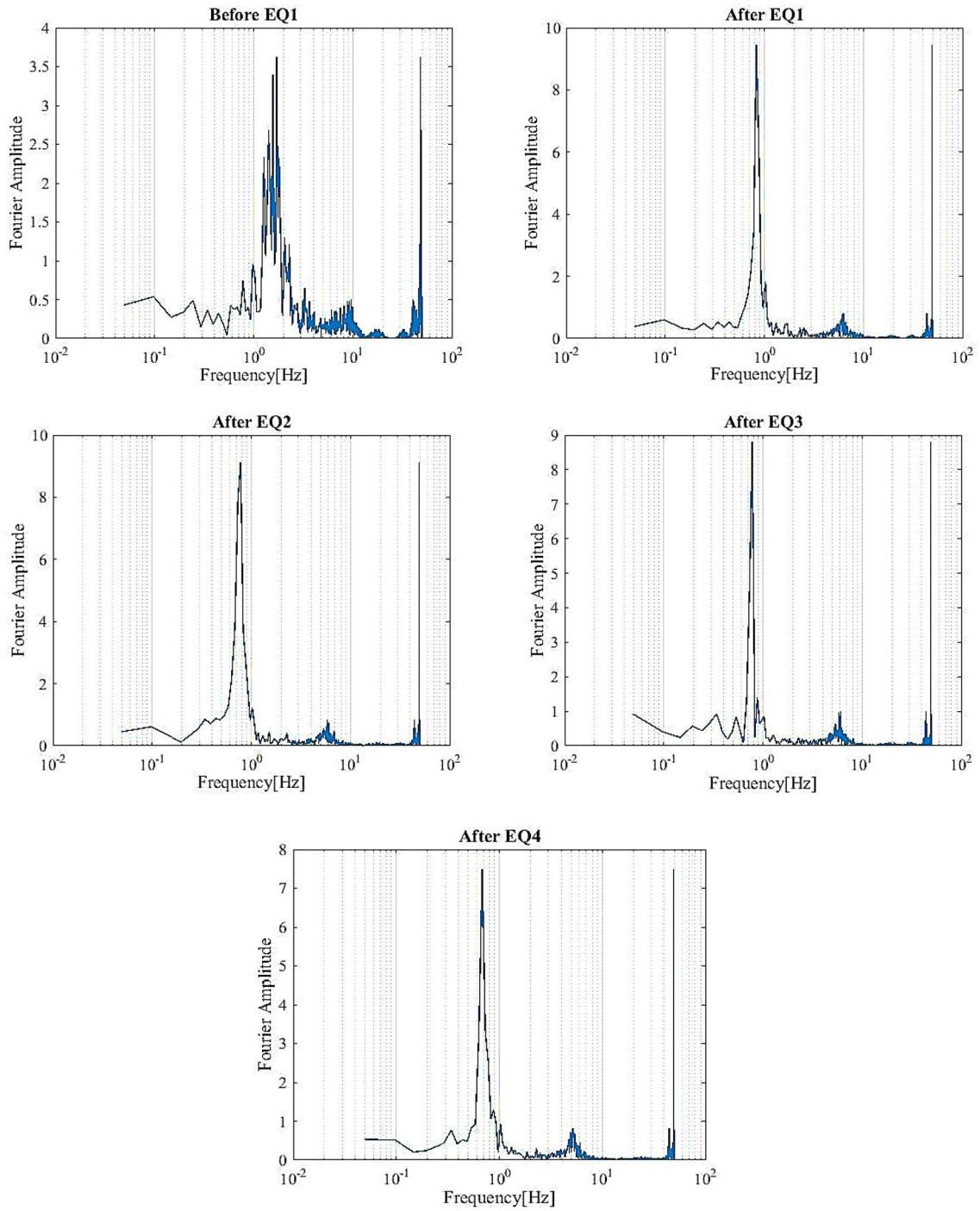


Fig. 28 Fourier spectrum before and after the earthquake—sixth level

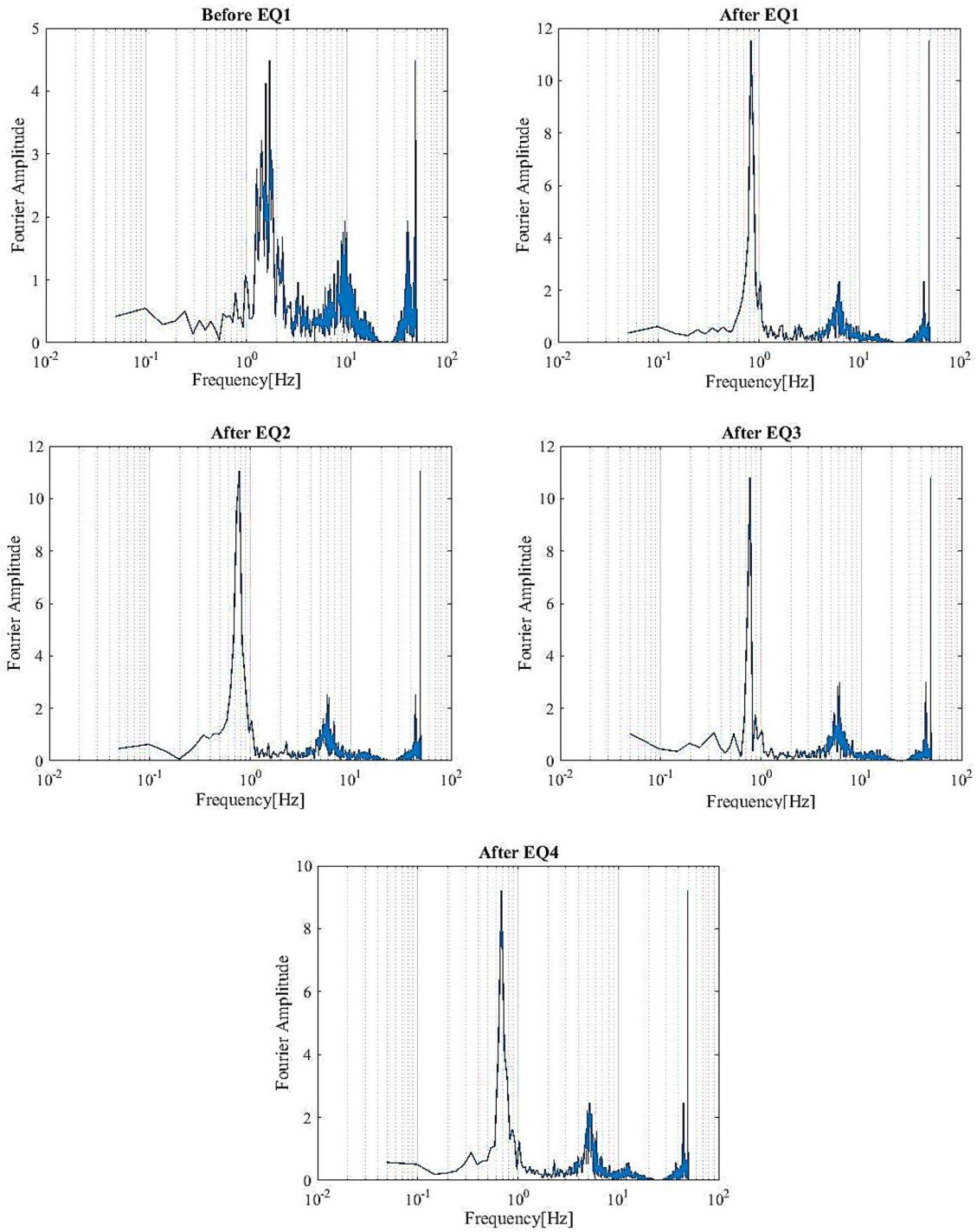


Fig. 29 Fourier spectrum before and after the earthquake—seventh level

Fig. 30 Fourier spectrum before and after the last earthquake—second level

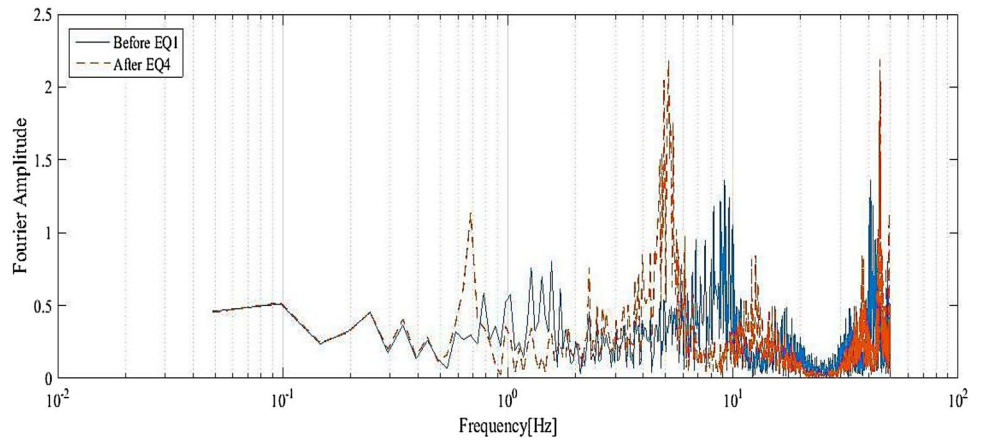


Fig. 31 Fourier spectrum before first and after last earthquake—third level

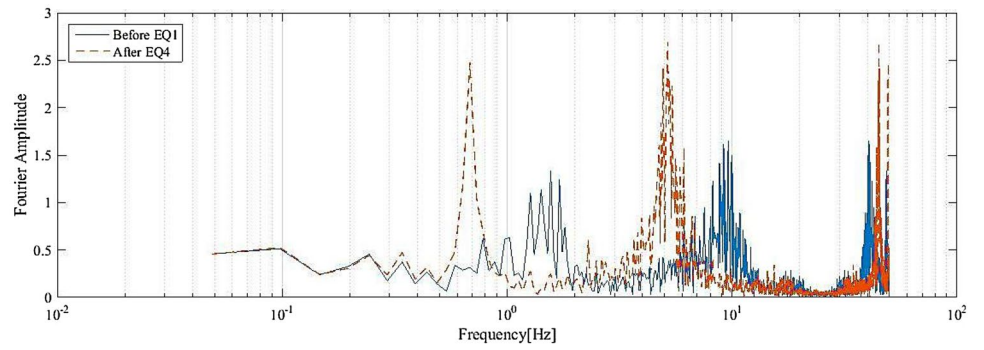


Fig. 32 Fourier spectrum before first and after last earthquake—fourth level

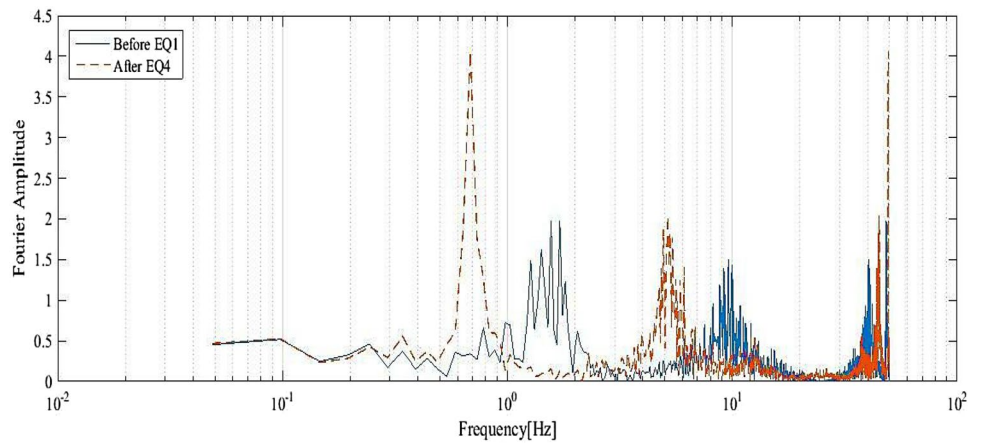


Fig. 33 Fourier spectrum before first and after last earthquake—fifth level

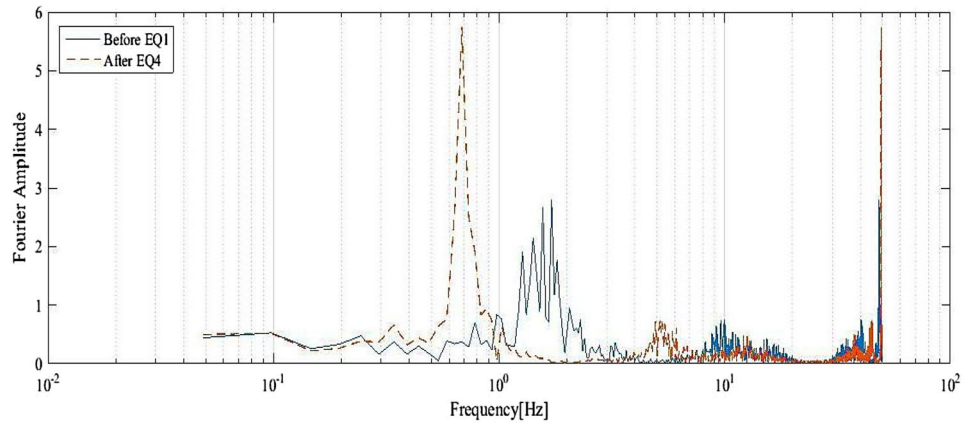


Fig. 34 Fourier spectrum before first and after last earthquake—sixth level

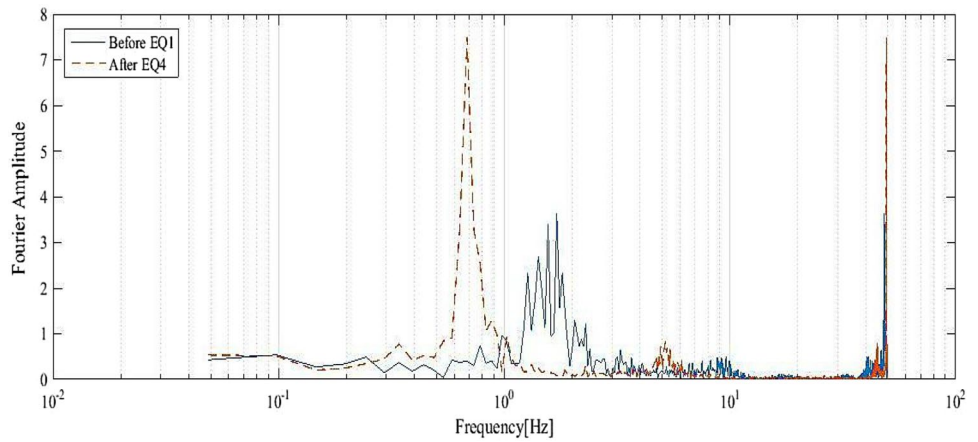
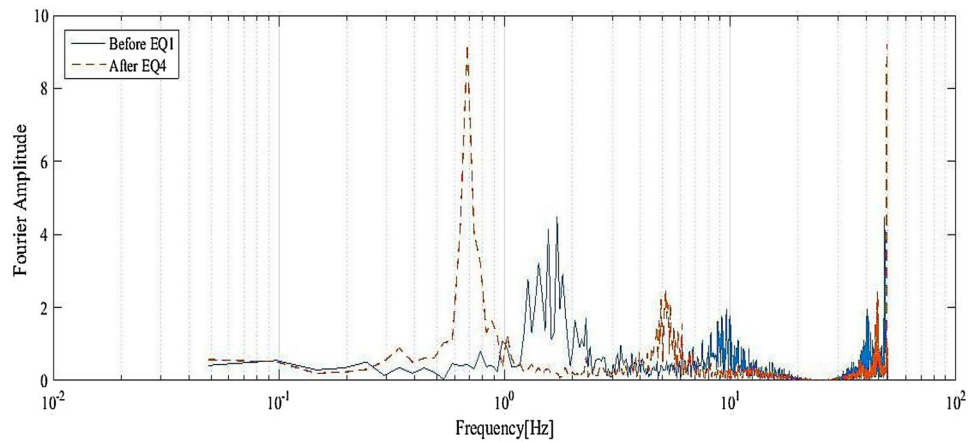


Fig. 35 Fourier spectrum before first and after last earthquake—seventh level



References

- Cawley P, Adams RD (1979) The location of defects in structures from measurements of natural frequencies. *J Strain Anal Eng Des* 14:49–57. <https://doi.org/10.1243/03093247V142049>
- Melhem H, Kim H (2003) Damage detection in concrete by Fourier and wavelet analyses. *J Eng Mech* 129:571–577. [https://doi.org/10.1061/\(ASCE\)0733-9399\(2003\)129:5\(571\)](https://doi.org/10.1061/(ASCE)0733-9399(2003)129:5(571))
- Ge M, Lui EM (2005) Structural damage identification using system dynamic properties. *Comput Struct* 83:2185–2196. <https://doi.org/10.1016/j.compstruc.2005.05.002>
- Sasmal S, Ramanjaneyulu K (2009) Detection and quantification of structural damage of a beam-like structure using natural frequencies. *Engineering* 01:167–176. <https://doi.org/10.4236/eng.2009.13020>
- Yan S, Sun W, Song G, Gu H, Huo LS, Liu B et al (2009) Health monitoring of reinforced concrete shear walls using smart aggregates. *Smart Mater Struct*. <https://doi.org/10.1088/0964-1726/18/4/047001>
- He K, Zhu WD (2011) Structural damage detection using changes in natural frequencies: theory and applications. *J Phys Conf Ser*. <https://doi.org/10.1088/1742-6596/305/1/012054>
- Barad KH, Sharma DS, Vyas V (2013) Crack detection in cantilever beam by frequency based method. *Procedia Eng* 51:770–775. <https://doi.org/10.1016/j.proeng.2013.01.110>
- Farhidzadeh A, Dehghan-Niri E, Salamone S, Luna B, Whittaker A (2013) Monitoring crack propagation in reinforced concrete shear walls by acoustic emission. *J Struct Eng*. [https://doi.org/10.1061/\(asce\)st.1943-541x.0000781](https://doi.org/10.1061/(asce)st.1943-541x.0000781)
- Vafaei M, Adnan A, AbdRahman AB (2013) Real-time seismic damage detection of concrete shear walls using artificial neural networks. *J Earthq Eng* 17:137–154. <https://doi.org/10.1080/13632469.2012.713559>
- Rezazadeh Eidgahee D, Fasihi F, Naderpour H (2015) Optimized artificial neural network for analyzing soil-waste rubber shred mixtures. *Sharif J Civ Eng* 31(2):105–111
- Mirrashid M (2017) Comparison study of soft computing approaches for estimation of the non-ductile RC joint shear strength. *Soft Comput Civ Eng* 1:12–28. <https://doi.org/10.22115/scce.2017.46318>
- Naderpour H, Rafiean AH, Fakharian P (2018) Compressive strength prediction of environmentally friendly concrete using artificial neural networks. *J Build Eng* 16:213–219. <https://doi.org/10.1016/j.jobe.2018.01.007>
- Naderpour H, Fakharian P (2017) Predicting the torsional strength of reinforced concrete beams strengthened with FRP sheets in terms of artificial neural networks. *J Struct Constr Eng* 5(1):20–35
- Rezazadeh Eidgahee D, Haddad A, Naderpour H (2018) Evaluation of shear strength parameters of granulated waste rubber using artificial neural networks and group method of data handling. *Sci Iran*. <https://doi.org/10.24200/sci.2018.5663.1408>
- Gokkus U, Yildirim M, Yilmazoglu A (2018) Prediction of concrete and steel materials contained by cantilever retaining wall by modeling the artificial neural networks. *J Soft Comput Civ Eng* 2:47–61. <https://doi.org/10.22115/scce.2018.137218.1078>
- Naderpour H, Rezazadeh Eidgahee D, Fakharian P, Rafiean AH, Kalantari SM (2019) A new proposed approach for moment capacity estimation of ferrocement members using group method of data handling. *Eng Sci Technol Int J*. <https://doi.org/10.1016/j.jestch.2019.05.013>
- Rezazadeh Eidgahee D, Rafiean AH, Haddad A (2019) A novel formulation for the compressive strength of IBP-based geopolymer stabilized clayey soils using ANN and GMDH-NN approaches. *Iran J Sci Technol Trans Civ Eng*. <https://doi.org/10.1007/s40996-019-00263-1>
- Fakharian P, Naderpour H, Haddad A, Rafiean AH, Rezazadeh ED (2018) A proposed model for compressive strength prediction of FRP-confined rectangular columns in terms of genetic expression programming (GEP). *Concr Res*. <https://doi.org/10.22124/jcr.2018.7162.1191>
- Naderpour H, Nagai K, Fakharian P, Haji M (2019) Innovative models for prediction of compressive strength of FRP-confined circular reinforced concrete columns using soft computing methods. *Compos Struct* 215:69–84. <https://doi.org/10.1016/j.compstruct.2019.02.048>
- Khiem NT, Toan LK (2014) A novel method for crack detection in beam-like structures by measurements of natural frequencies. *J Sound Vib* 333:4084–4103. <https://doi.org/10.1016/j.jsv.2014.04.031>
- Lin RM (2016) Modelling, detection and identification of flexural crack damages in beams using frequency response functions. *Meccanica* 51:2027–2044. <https://doi.org/10.1007/s11012-015-0350-6>
- Naderpour H, Fakharian P (2016) A synthesis of peak picking method and wavelet packet transform for structural modal identification. *KSCE J Civ Eng* 20:2859–2867. <https://doi.org/10.1007/s12205-016-0523-4>
- Naderpour H, Ezzodin A, Kheyroddin A, Ghodrati Amiri G (2017) Signal processing based damage detection of concrete bridge piers subjected to consequent excitations. *J Vibroeng* 19:2080–2089. <https://doi.org/10.21595/jve.2015.16474>
- Haddad A, Rezazadeh Eidgahee D, Naderpour H (2017) A probabilistic study on the geometrical design of gravity retaining walls. *World J Eng* 14:414–422. <https://doi.org/10.1108/WJE-07-2016-0034>
- Ghasemi SH, Nowak AS (2017) Target reliability for bridges with consideration of ultimate limit state. *Eng Struct* 152:226–237. <https://doi.org/10.1016/j.engstruct.2017.09.012>
- Ghasemi SH, Nowak AS (2017) Reliability index for non-normal distributions of limit state functions. *Struct Eng Mech* 62:365–372. <https://doi.org/10.12989/sem.2017.62.3.365>
- Ghasemi SH, Nowak AS (2018) Reliability analysis of circular tunnel with consideration of the strength limit state. *Geomech Eng* 15:879–888. <https://doi.org/10.12989/GAE.2018.15.3.879>
- Bradley BA, Burks LS, Baker JW (2015) Ground motion selection for simulation-based seismic hazard and structural reliability assessment. *Earthq Eng Struct Dyn* 44:2321–2340. <https://doi.org/10.1002/eqe.2588>
- Hosseini P, Ghasemi SH, Jalayer M, Nowak AS (2019) Performance-based reliability analysis of bridge pier subjected to vehicular collision: extremity and failure. *Eng Fail Anal* 106:104176. <https://doi.org/10.1016/j.engfailanal.2019.104176>
- Moaveni B, Conte JP (2014) System and damage identification of civil structures. *Encycl Earthq Eng*. https://doi.org/10.1007/978-3-642-36197-5_70-1

Publisher's Note Springer Nature remains neutral with regard to jurisdictional claims in published maps and institutional affiliations.